Available online at www.sciencedirect.com
SCIENCE DIRECT
Polymer 46 (2005) 9562–9573
polymer
www.elsevier.com/locate/polymer

Termination rate coefficients for acrylamide in the aqueous phase at low conversion

Shane A. Seabrook, Philippe Pascal, Matthew P. Tonge, Robert G. Gilbert*

School of Chemistry F11, Key Center for Polymer Colloids, The University of Sydney, Sydney, NSW 2006, Australia

Received 6 July 2005; received in revised form 21 August 2005; accepted 22 August 2005
Available online 13 September 2005

Abstract

The kinetics of acrylamide (AAm) free radical polymerization at low conversion of monomer to polymer in the aqueous phase was investigated at 50 °C using γ-radiolysis relaxation, which is sensitive to radical-loss processes. The values of the termination rate coefficients for AAm ranged from 8×10^6 to 3×10^7 M^{-1} s^{-1} as the weight fraction of polymer ranged from 0.002 to 0.0035, which is significantly lower than the low-conversion values for monomers such as styrene (2×10^8 M^{-1} s^{-1}) and methyl methacrylate (4×10^7 M^{-1} s^{-1}) in organic media. These can be quantitatively explained by applying a chain-length-dependent model of free-radical polymerization kinetics [Russell GT, Gilbert RG, Napper DH. Macromolecules 1992;25:2459. [19]] in which termination kinetics are expressed in terms of a diffusion-controlled encounter of radicals which ultimately yields an expression for the chain-length-averaged termination rate coefficient, $\langle k_t \rangle$. The lower $\langle k_t \rangle$ for AAm arises due to a combination of the high k_p value, promoting rapid formation of slower terminating long chains, and the slow diffusion of short propagating chains, relative to other common monomers. The chain transfer to monomer constant for AAm in water at 50 °C, C_M, was estimated using the chain-length-distribution method with correction for band-broadening [Castro JV, van Berkel KY, Russell GT, Gilbert RG. Aust J Chem 2005;58:178. [21]] and found to be 1.2×10^{-4} (±10%). The diffusion characteristics for AAm were adapted from those obtained for a similar aqueous system (hydroxyethyl methacrylate) together with a 0.5 exponent for the power law dependence on penetrant degree of polymerization at zero weight fraction polymer. This provides an adequate fit to the $\langle k_t \rangle$ data. This is the first application of the chain-length-dependent model to describe experimental termination rate coefficients for an aqueous system at low conversion to polymer. The result that the experimental termination rate coefficients can be reproduced with an a priori model with physically reasonable parameters supports the physical assumptions underlying that model.

Keywords: Acrylamide; Termination; Relaxation

1. Introduction

The aqueous phase polymerization of acrylamide (AAm) is involved in many commercial products [1], importantly flocculating agents and gel electrophoresis [2], and a better understanding of the complex events that occur during polymerization is important for refinement of the current products, and indeed for the efficient design of novel products. The aqueous phase polymerization of AAm can take place in a solution or in a more complex multi-phase process such as inverse emulsion; the present study is confined to a homogeneous aqueous system.

Polyacrylamide (PAAm) is distinguished from other non-ionic polymers by its highly hydrophilic character and relatively large molecular weights (in industry usually $> 10^7$), which makes each chain highly expanded when saturated with water. For example, PAAm with a MW of 10^6 has a root-mean-square end-to-end distance $\langle r^2 \rangle^{1/2} \approx 170$ nm [3], which is large compared to polystyrenes of the same molecular weight where $\langle r^2 \rangle^{1/2} \approx 74$ nm. This character is reflected in the large Mark–Houwink exponent of 0.80 in water [1]. Moreover, like other hydrophilic monomers [4–9], it has an extremely high propagation rate coefficient which is very sensitive to changes in the solvent (water) [9].

The measurement of termination rate coefficients is fraught with difficulties, and the origins of the inconsistencies

* Corresponding author. Tel.: +61 2 9351 3366; fax: +61 2 9351 8651.
E-mail address: gilbert@chem.usyd.edu.au (R.G. Gilbert).

0032-3861/$ - see front matter © 2005 Elsevier Ltd. All rights reserved.
doi:10.1016/j.polymer.2005.08.062

in the literature, and the advantages and disadvantages of different techniques, has been examined by an IUPAC Working Party [10,11]. There have been important advances in using the techniques of controlled-radical polymerization to measure (average) termination rate coefficients in systems where both terminating chains are of approximately the same degree of polymerization ('long-long' termination, see for example [12,13]). In the present study, we examine a conventional initiation system, where the termination events are dominated by reactions between short and long chains: 'short-long termination' (i.e. the radical populations, and hence $\langle k_t \rangle$, are different in the controlled-radical techniques and the conventional ones which are the subject of the present work).

Until recently, kinetic studies on acrylamide polymerization had involved data where initiation, propagation and termination occurred simultaneously. This made it nearly impossible to provide unambiguous qualitative evidence for the values of these rate coefficients and the physical events controlling them, as each of these kinetic events is complex in its own right. Advances in experimental technology have provided techniques that supply data which are sensitive to only one of the separate processes; in the present paper data are interpreted from polymerizations initiated using γ-radiolysis, with subsequent analysis of the relaxation behavior (kinetics following removal from the initiation source). Such data are especially sensitive to the radical-loss process [14–17], which in the case of acrylamide polymerization in the aqueous phase correlates directly to termination. For a full interpretation of the termination kinetics we use a previous study of AAm polymerization which employed strategies which were sensitive largely to aqueous-phase propagation in isolation [9] (using the technique of pulsed-laser polymerization).

Termination rate coefficients $\langle k_t \rangle$ were obtained at low conversion by measuring the relaxation kinetics with automated dilatometry. The time resolution of the device (e.g. one reading every 5 s) used here enabled detailed tracking of the rapid kinetics displayed by polymerizing AAm. Consequently, a number of unusual phenomena associated with the kinetic relaxations will be seen to be revealed by this method, providing insights for diffusion-controlled polymerization termination kinetics in general.

The $\langle k_t \rangle$ data obtained here are interpreted in terms of a well-accepted scheme where termination rate coefficients are dependent on the lengths of the terminating chains [16,18,19], a dependence which can be very strong under typical polymerization conditions. This recognizes the important contribution to termination by relatively mobile short-chain radicals. The model is applied at infinite polymer dilution for aqueous AAm. This model depends inter alia on the value of the rate coefficient for transfer to monomer, which was determined in independent experiments from the molecular weight distributions (MWDs) obtained under appropriate conditions, using the 'number distribution' method [20] with corrections for band broadening [21,22].

The quantitative model used here describes the complete evolution of the population of each degree of polymerization [17,19]. It is often convenient to define an average termination rate coefficient $\langle k_t \rangle$, an average over all radical chain lengths:

$$\langle k_t \rangle = \frac{\sum_i \sum_j k_t^{ij} T_i T_j}{\left(\sum_i T_i\right)^2} \tag{1}$$

where k_t^{ij} is the termination rate coefficient between chains of degree of polymerization i and j, and T_i is the population of radicals of degree of polymerization i. The full evolution equations for bulk or solution polymerization then result in the rate equation:

$$\frac{d[R^\cdot]}{dt} = 2k_d f[I] - 2\langle k_t \rangle [R^\cdot]^2 \tag{2}$$

where $[R^\cdot] = \sum T_i$ is the total radical concentration, k_d the initiator dissociation rate coefficient and f the initiator efficiency. It is essential to be aware that $\langle k_t \rangle$ will in general depend on the polymer weight fraction in the system (w_p) but in addition will also depend (through the T_i) on initiator concentration, system history, etc. Thus $\langle k_t \rangle$ will be expected in general to depend on time and on $[R^\cdot]$: that is, Eq. (2) can only be solved given the complete time-evolution of the T_i, whose defining equations are given below. Termination kinetics is frequently treated without taking chain-length dependence into account. In fact, the value of $\langle k_t \rangle$ is actually defined from Eq. (2) and can be deduced from experiment by fitting of the data to this functional form. A generally applicable means of determining $\langle k_t \rangle$ is from knowledge of the conversion in an experiment as a function of time:

$$\frac{d[M]}{dt} = -k_p [M][R^\cdot] \tag{3}$$

where [M] is the monomer concentration in the locus of polymerization.

Because of Eq. (1), interpreting kinetic data with Eq. (2) will yield an 'instantaneous' termination rate coefficient which may be dependent on time, system history, etc. although the resulting $\langle k_t \rangle$ will exactly (but trivially) reproduce the observed instantaneous rate under the specified conditions at the specified instant. Nevertheless, Eq. (2) is a convenient intermediate step in data interpretation, and will be used to give instantaneous $\langle k_t \rangle$ values for AAm which can then be compared to those for other monomers and from theory.

2. Experimental

2.1. Reagents

AAm (Aldrich, electrophoresis grade 99%); uranyl nitrate (Ajax Chemicals, 99%); and hydroquinone (Aldrich, 99%) were used as received. Doubly distilled water (second

distillation over alkaline permanganate) was used as solvent throughout, except for the transfer to monomer experiment, where Milli-Q water (Milli-Q Plus 18.2 Ω filtration) was used.

2.2. Dilatometry

Kinetic data were obtained by automated dilatometry. The contraction factor c_f which relates height change to conversion ($c_f = d_{M^{-1}} - d_{P^{-1}}$, where d_M and d_P are the densities of pure monomer and polymer, respectively) was taken as 0.22 $cm^3\ g^{-1}$ at 50 °C [23], and conversions so obtained checked with gravimetry. All experiments were conducted using ~0.45 M AAm in water, the actual values for each being shown in Table 1.

2.3. γ-Radiolysis

γ-Radiation using a cobalt-60 source (which emits two γ quanta of energies 1.173 and 1.332 MeV) provides a means whereby initiation may be activated or de-activated at any time, regardless of the stage of polymerization. This was accomplished by inserting or removing a dilatometric reaction vessel, together with a meniscus tracking device. Removal of the dilatometer from this source which will effectively stop any initiation, allowing the polymerization to relax. An instantaneous value of $\langle k_t \rangle$ can be obtained through Eq. (2). Provided k_p is known, and under γ-radiolysis relaxation conditions where there is no source of free radicals (i.e. assuming that thermally-generated radicals can be ignored), the following equation, derived from Eqs. (2) and (3), was fitted to the resultant decay to obtain $\langle k_t \rangle$:

$$\frac{d[M]}{dt} = \left(\frac{d[M]}{dt}\right)_0 \left\{ \frac{\left(\frac{d[M]}{dt}\right)_0 \langle k_t \rangle t}{[M]_0 k_p} + 1 \right\}^{(-(k_p/\langle k_t \rangle)-1)} \quad (4)$$

where the subscript 0 refers to the value of the quantity at the start of the decay ($t=0$). The data fitting was carried out by a Simplex least-squares fit to Eq. (4), using numerical differentiation of the experimental conversion/time data and our experimental value of k_p for the conditions under study [9].

Because the relaxation kinetics depend on the initiator concentration and system history, it is necessary to provide details of the radical flux used in the present experiments: i.e. the G value. In our data manipulation, the radical production rate is fitted to the observed initial rate, thereby generating the requisite population of radicals of a given degree of polymerization explicitly, without need for a separate knowledge of the initial radical flux, but the following details are given so that it is possible for an independent reproduction of our experimental data.

The major constituent of the polymerization mixture in this work is water (96.5%). Consequently, the major source of primary free radicals is from the irradiation of water. Ignoring the relatively short-lived intermediate species, the radical species that are possibly capable of initiating polymerization reactions are [24]:

$$H_2O \longrightarrow HO^{\bullet}, H^{\bullet}, e^-_{aq} \quad (5)$$

The G value is the number of product molecules formed for each 100 eV of γ-energy absorbed by the system. The two major radical species formed in γ-irradiation of water are [24] $HO^{\bullet}$ ($G=2.8$) and hydrated electrons, e^-_{aq}, ($G=2.7$); hydrogen atoms ($G=0.55$) is a minor component. For γ-radiation of concentrations of AAm between 0.05 to at least 0.7 M, at neutral pH, the G value for the number of polymerization chains initiated has been reported to range from that of pure water (6.05) to about 7.5 [25]. These G values may indicate that AAm molecules are also contributing to primary radical production, but the magnitude of this production is not certain because the authors did not specify how the number of polymerization chains were counted.

All reaction solutions were de-oxygenated prior to charging the dilatometer by heating to about 50 °C, followed by a number of alternate applications of vacuum and nitrogen gas sparging. The time taken for the dilatometer to be removed from the γ-source was less than 6 s. This study used three dose rates. Taking into account the half-life of ^{60}Co (5.26 y) and a reasonable value of G (6.05), the corresponding rates of primary free radical production were estimated, given in Table 1.

2.4. Molecular weights

Size exclusion chromatography (SEC) incorporating universal calibration was used to determine the peak MW

Table 1
Conditions and $\langle k_t \rangle$ values for γ-radiolysis relaxation experiments

Experiment code	Exp1	Exp2	Exp3
Dose rate (mGy s^{-1})	7.25	37.2	220
Radical production rate (M s^{-1})	4.55×10^{-9}	1.93×10^{-8}	1.38×10^{-7}
x_0	0.058	0.090	0.100
x_f	0.065	0.110	0.135
$[M]_0$ (M)	0.467	0.436	0.447
$[R^{\bullet}]_0$ (M)	1.29×10^{-7}	1.58×10^{-7}	3.49×10^{-7}
M_p	1.33×10^{6}	1.25×10^{6}	0.70×10^{6}
$\langle k_t \rangle$ ($M^{-1}\ s^{-1}$)	3×10^{7}	1×10^{7}	8×10^{6}

of PAAm at the end of relaxation experiments. Measurements employed a Waters M-6000A chromatograph with an ultrahydrogel-linear column. Narrow polydispersity poly (ethylene oxide) standards (Toyo Soda, molecular weight range 1.8×10^4–9.9×10^5) were used for universal calibration with the Mark–Houwink parameters being $K=4.9\times10^3$ cm^3 g^{-1} and $\alpha=0.80$ [1,26–28].

2.5. Transfer constant

The transfer constant of AAm to PAAm, C_M, was determined using the chain-length-distribution method [20,22,29] by polymerizing a series of AAm solutions (0.400 M) with decreasing concentration of the photoinitiator uranyl nitrate (0.0050–0.0005 M). Uranyl nitrate was chosen, as it is easy to control polymerization via UV light. Ideally, conversion should be less than 10%; this was routinely checked using a Renishaw dispersive Raman spectrophotometer, with an excitation wavelength of 514 nm. MWDs were measured using aqueous-phase SEC incorporating absolute molecular weight detection via multi-angle laser light scattering (MALLS). PSS Suprema 100 and 30,000 columns were used on a Shimadzu SEC unit, in line with a Wyatt 18 angle MALLS and a Dawn differential refractometer, at a flow rate of 0.4 mL min^{-1}.

The 'number distribution' method to obtain the transfer constant is based on the result [20] that the number MWD $P(M)$ (the number of chains with molecular weight M) in free-radical polymerization formed at a particular conversion (i.e. the instantaneous MWD) can be very accurately approximated by a simple exponential form:

$$P(M) = \exp(-\Lambda M) \tag{6}$$

where Λ is a simple function of the various rate coefficients controlling the kinetics (see below). The number MWD $P(M)$ in turn is related to the SEC distribution $w(\log M)$ (which is the 'ideal' distribution that would be obtained from size-exclusion chromatography with linear calibration and in the absence of band broadening) by [20,30]:

$$P(M) = M^{-2}w(\log M) \tag{7}$$

Hence, the value of Λ, and hence the desired rate coefficients, can be obtained from the slope of a plot of ln $P(M)$ against molecular weight. In determining $w(\log M)$ and hence $P(M)$ from the experimental SEC trace, it is essential to take band broadening into account, for which we use a recently developed methodology [21,22]. This methodology employs the result that the slope of the true, i.e. 'unbroadened', ln $P(M)$ of the form of Eq. (6) is the same of that of the ln $P(M)$ inferred from the experimental $w(\log M)$, without taking account of band broadening at the maximum in the experimental (broadened) $w(\log M)$.

The transfer constant to monomer, C_M, is estimated from the appropriate form of the equation describing the dependence of the slopes (ΛM_0) of ln $P(M)$ [20]:

$$\Lambda M_0 = C_M + \frac{\langle k_t\rangle (f k_d[I])^{1/2}}{2k_p[M]} \tag{8}$$

The form of Eq. (8) shows that C_M can be obtained by plotting the values of Λ for a series of initiator concentrations [I] against [I]$^{1/2}$: the intercept then gives C_M.

3. Experimental results

3.1. Termination rate coefficients

Three different dose rates were utilized for initiating polymerization. Data from the first relaxation experiment (exp1) are represented as the rate of polymerization in Fig. 1. Two more experiments were conducted at different

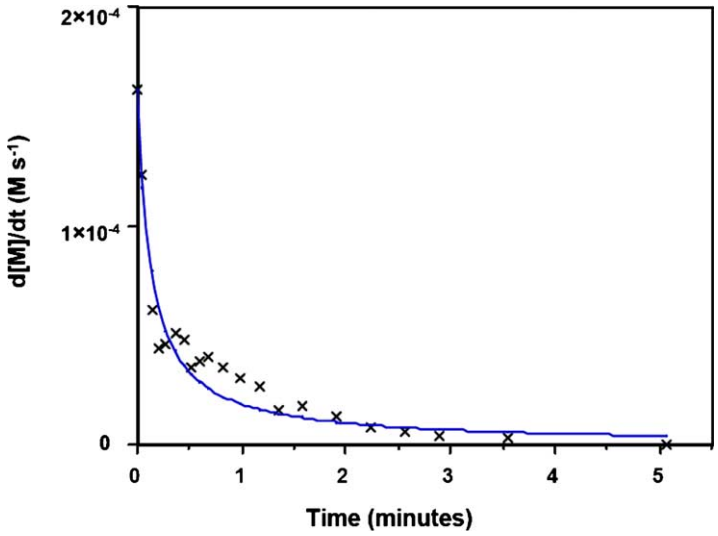

Fig. 1. Kinetic relaxation results for exp1: experiment (crosses); and the fitted model (line). Temperature = 50 °C, [M] = 0.467 M.

dose rates (exp2 and exp3, rates not illustrated; dose rates given in Table 1).

The line in Fig. 1 is the fit based upon Eq. (2) obtained by optimizing a $\langle k_t \rangle$ value for an entire relaxation. The optimization for all relaxations was carried out using the k_p values shown in Table 1, as measured by pulsed-laser polymerization for this system [9]. By repeating experiment exp2 twice more under identical conditions, the precision of $\langle k_t \rangle$ was estimated as $\pm 10\%$. The value of $\langle k_t \rangle$ at the start of the relaxation, $\langle k_t \rangle_0$, was obtained by fitting the data to Eq. (2) at a series of different times throughout the relaxation and extrapolating to $t=0$; the instantaneous values of $\langle k_t \rangle$ are shown in Fig. 2 for the 5 min relaxation. Table 1 summarizes the resultant values of $\langle k_t \rangle$ along with some experimental conditions under which these values were determined: x_0 and x_f = fractional conversion of monomer at the start and end of the relaxation; $[M]_0$ = initial monomer concentration $[M]_0$, $[R^{\cdot}]_0$ = radical concentration calculated from experimental rate and Eq. (3), M_p = peak molecular weight of polymer at the end of the relaxation as determined by SEC.

The value of x_0 for each dose rate was selected such that the rate of polymerization was at its greatest, which also corresponded to a brief 'steady-state' plateau. Examples of the rate (dx/dt as a function of x) are shown for exp4 in Fig. 3. Exp4 was performed under equivalent conditions to exp1, except that it was not removed from the γ-source. The corresponding conversion-versus-time curve for exp4 is shown in Fig. 4.

There is an apparent peculiarity in the relaxation results: if each experimental relaxation is fitted with a single value of $\langle k_t \rangle$ (using Eq. (2)) such that the experimental $d[M]/dt$ can be replicated as well as possible by a least-squares fit, these fitted $\langle k_t \rangle$ values tend to increase very slightly with relaxation time (Fig. 2). However, in all cases we would expect the $\langle k_t \rangle$ value to decrease with time due to propagating chains increasing in chain length with termination becoming diffusion-controlled [31–33]. Now, the apparent oscillations in the k_t values at early times simply reflect the noise in the data, and it should be recalled that the values of $\langle k_t \rangle$ reported in Table 1 are the limiting values of these instantaneous $\langle k_t \rangle$ at the start of relaxation. Although this is reasonable as a first approximation, it is indeed apparent that fitting the experimental curves in this manner is not perfectly adequate (Fig. 1). It is likely that this anomaly is due to a small effect of the exotherm during the reaction, to which dilatometry is extremely sensitive. The anomaly is visible as a rate of change of a rate of change, i.e. effectively the second derivative of the raw data. While it is possible to correct for this artifact [34], this correction is extremely difficult to do for the present system since acceptable accuracy can only be obtained [34] by running the reaction at much lower temperatures than used here (chosen because of practical applications).

As expected, the $\langle k_t \rangle$ values decrease with increasing conversion (weight fraction polymer), illustrated in Table 1.

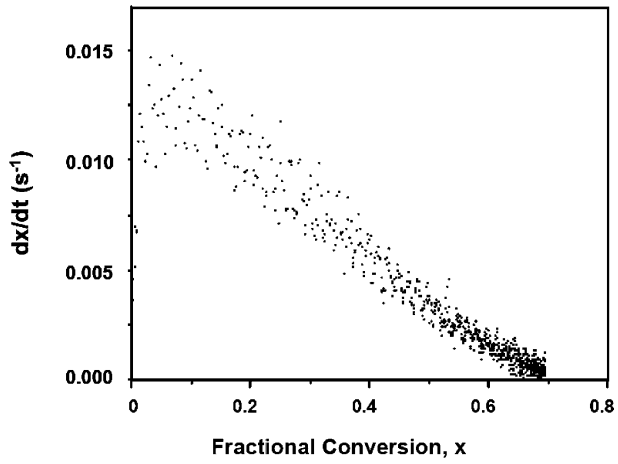

Fig. 3. Rate of polymerization for exp4, which was performed under the same conditions as exp1, except it was not removed from the γ source.

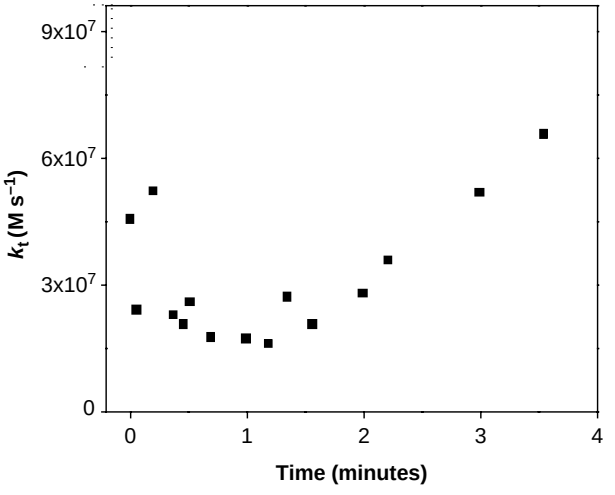

Fig. 2. Values of k_t fitted to the rate of relaxation for every datum in time (exp1). Temperature = 50 °C, [M] = 0.467 M.

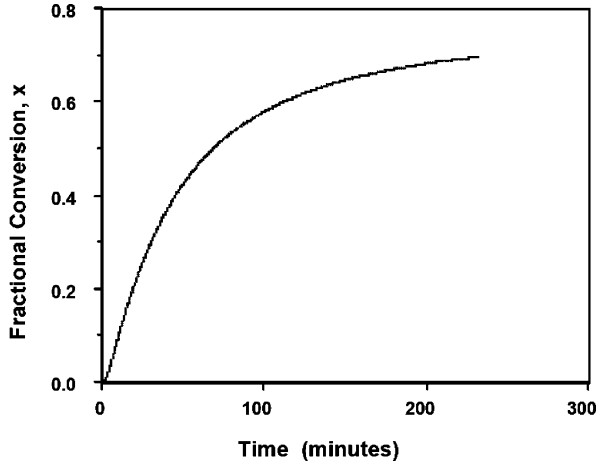

Fig. 4. Conversion curve corresponding to experiment exp4.

Also, comparison of $\langle k_t \rangle$ values for AAm with those at low conversion for systems such as styrene and methyl methacrylate indicates that, despite the high scatter in literature values [11], those for AAm are an order of magnitude lower.

This major difference between termination rate coefficients for acrylamide and typical hydrophobic monomers is ascribed here to effects of chain-length-dependent termination. This is a result of a combination of relatively fast propagation of short radicals to form longer, more slowly diffusing (and terminating) radicals, and the relatively slow diffusion of the polar AAm oligomers. This general trend is also seen in compilations of termination rate coefficients [35], although it is essential to be aware [36–38] that this compilation was not critically evaluated and contains many internal inconsistencies.

3.2. Transfer constants

The MWDs as SEC distributions and ln $P(M)$ plots obtained from the transfer to monomer experiments are shown in Fig. 5. As stated, the exponential form of $P(M)$ predicted by Eqs. (6) and (8) is masked by the occurrence of band broadening [39]. It has been proved [39,40] that the slope from the experimental (broadening-affected) ln $P(M)$ plots corresponding to the peak of the MWDs is also the value of the true, unbroadened, ln $P(M)$. These slopes plotted against the square root of uranyl nitrate (initiator) concentration, from which the intercept provides a value for C_M ($=k_{tr}/k_p$) of 1.2×10^4 (with an uncertainty of 10%), shown in Fig. 6. This value is similar to those of other monomers at 50 °C: styrene (2.8×10^4 [41]), butyl acrylate (2.8×10^4 [42,43]) and methyl methacrylate (8.6×10^4 [44]). It should be noted that the MWDs from which this is derived do not all appear to be unimodal distributions, which suggests that there may be kinetically significant events occurring that are not taken into account. However, the trend of a decreasing slope on the ln $P(M)$ plots at the point which corresponds to the maximum molecular weight from the MWD still holds true.

The value of k_{tr} is relatively high, and it is not obvious which abstraction reaction is responsible for this. However, this process is one that occurs in the water phase, and the presence of this solvent produces very large effects on free energies of activation for these radical processes [45]. A comparison between rate coefficients for transfer reactions in organic and aqueous solvents requires extensive data on the Arrhenius parameters for these processes for meaningful understanding.

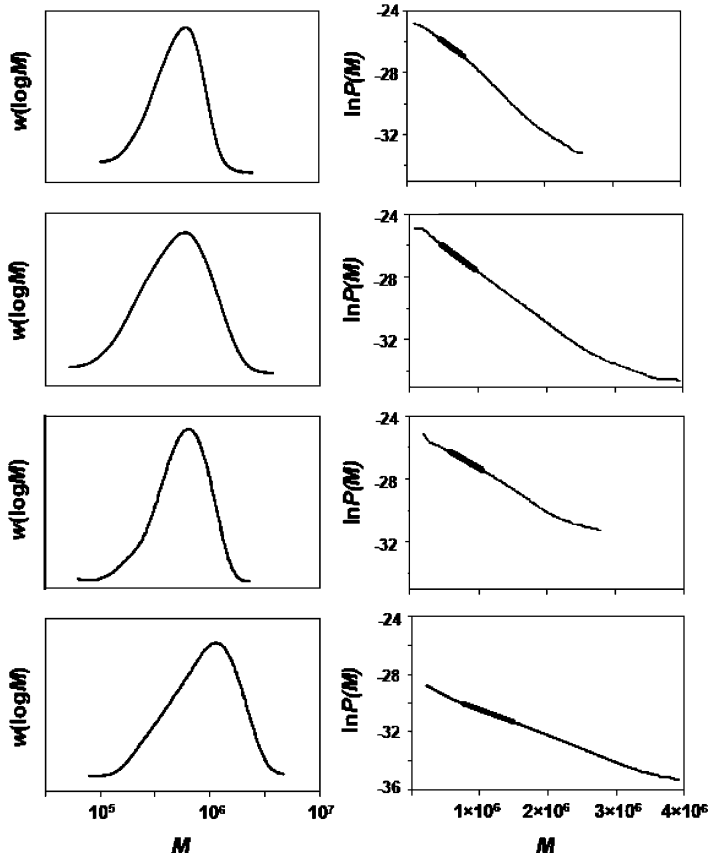

Fig. 5. MWDs and corresponding ln $P(M)$ plots from chain transfer to monomer experiments. The heavy solid line is a fitted straight line taken from the MW corresponding to the peak on the MWD.

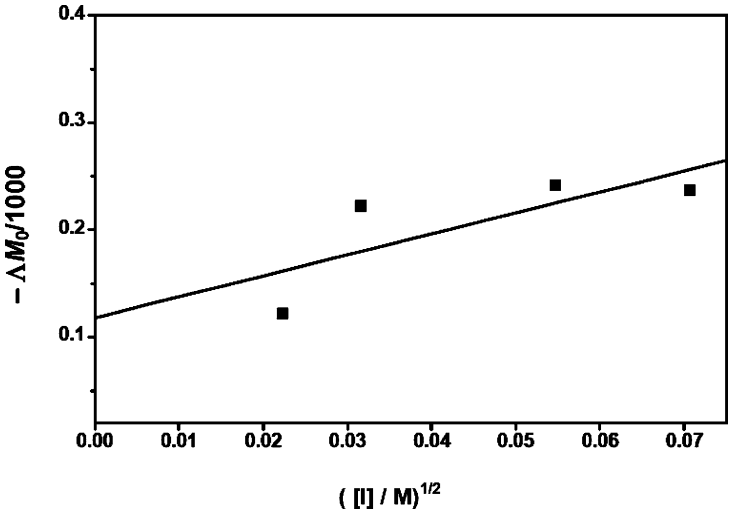

Fig. 6. Slope of the ln $P(M)$ plot at the point corresponding to the maximum from the MWDs versus the square root of the initiator concentration. The intercept yields a value for C_M which is equal to k_{tr}/k_p.

4. Chain-length-dependent termination

4.1. Parameters

It has been conclusively shown by examination of sensitive experimental data [16,46,47] that termination kinetics in experiments, such as the present type (relaxation) which are sensitive to termination mechanism, cannot be consistently fitted by 'classical' second-order loss termination kinetics with a generic k_t. The values can be interpreted by taking account of the dependence of the termination rate coefficients on chain length. Modeling sensitive relaxation data [16], where radical loss is dominated by termination, has provided firm experimental evidence of the long-recognized [11,18,19,31–33,48–56] phenomenon that termination kinetics depend on the degrees of polymerization i and j of the two chains involved, and thus the termination rate coefficient must be written k_t^{ij}. In this section, we give an overview of the model needed for understanding the present data. The model is expressed in terms of the time evolution of the population of free radicals of degree of polymerization i, T_i. The kinetic events, which must be taken into account, are propagation, transfer, initiation and chain-length dependent termination. The resulting evolution equations are:

$$\frac{dT_1}{dt} = 2k_d f[I] + k_{tr}[M]\sum_{i=2}^{\infty} T_i - k_p^1[M]T_1 - 2T_1\sum_{i=1}^{\infty} k_t^{1i}T_i \quad (9)$$

$$\frac{dT_i}{dt} = -k_{tr}[M]T_i + [M]\left(k_p^{i-1}T_{i-1} - k_p^i T_i\right) - 2T_i\sum_{j=1}^{\infty} k_t^{ji}T_j, \quad i>2 \quad (10)$$

Here [M] is the monomer concentration in the locus of polymerization, k_{tr} is the rate coefficient for transfer to monomer (other types of transfer are here ignored), and k_p^i is the rate coefficient for propagation, which may in general be dependent upon the degree of polymerization i of the propagating radical. For γ-radiolysis relaxation conditions, the initiation term is absent following removal from the radiation source. Chain transfer to polymer is ignored. For AAm, chain transfer to the solvent (water) is also insignificant [57].

Eqs. (9) and (10) can be simplified through the steady-state approximation, which yields a set of non-linear equations which are exactly solved iteratively [20] to yield each T_i. In the present simulations, these non-linear equations are solved exactly by numerical means detailed elsewhere [20]. In solving Eqs. (9) and (10), it is necessary to specify fk_d, to which the computed $\langle k_t\rangle$ is only slightly sensitive. For γ-radiolysis relaxation, this was done by choosing $fk_d[I]$ to give the observed polymerization rate at the moment of removal from the radiation source, i.e. the $fk_d[I]$ terms in Table 1 were chosen to match the radical flux terms in Table 1. For this reason, the value of the composite term $fk_d[I]$ was not varied in the simulations below.

We now specify the functional forms and parameters employed for the simulations. The microscopic termination rate coefficients are found starting with the Smoluchowski equation:

$$k_t^{ij} = 2\pi p D_{ij}\sigma \quad (11)$$

Here, D_{ij} is the mutual diffusion coefficient for diffusion of the radical ends of an i-mer and a j-mer, p is the probability of reaction upon encounter, which may less than one because of the effects of spin multiplicity [17], and σ is the Lennard–Jones diameter of a monomer unit. The Lennard–Jones diameter can be defined from

$$\sigma = r_i + r_j \tag{12}$$

where $(r_i + r_j)$ are the radii of interaction for termination. The value for σ was taken from an earlier study [58]. The spin multiplicity factor p takes account of the fact that each radical (being a doublet) can be in one of two possible spin states. The probability is thus 1/4 that two free radicals will have opposite spin and so be able to combine (combining identical spins gives three possible triplet states, while there is only one singlet state possible when combining opposite spins). Hence the effective encounter rate coefficient given by the Smoluchowski equation might need reduction by a factor of 4, i.e. $p = 1/4$. However, in the condensed phase, especially with regards to relatively slow termination, two adjacent free radical ends may be trapped within a solvent cage sufficiently long to allow the spins to flip, when one would have $p = 1$. In a glassy polymeric system, it is reasonable to put $p = 1$. The value of p at low conversions is unknown, but following earlier studies [17] that suggested that $p = 1/4$ gave the most consistent fit for termination kinetics in methyl methacrylate at intermediate conversion, we adopt the same value here for all systems studied at low conversion. We note that p always appears as the product pD_{mon} (where D_{mon} is the diffusion coefficient of a monomer radical—see below), so that these two quantities, although physically quite distinct, comprise only a single unknown parameter whose value can be estimated from independent information [17] within narrow limits. The mutual diffusion coefficient D_{ij} is the sum of contributions from the two reacting species:

$$D_{ij} = D_i + D_j \tag{13}$$

There are two components to each D_i: centre-of-mass diffusion of the chain as a whole, with diffusion coefficient D_i^{com}, and diffusion by propagational growth of the chain end ('reaction–diffusion'), with diffusion coefficient D^{rd} (this quantity is independent of chain length). Hence:

$$D_i = D_i^{\mathrm{com}} + D^{\mathrm{rd}} \tag{14}$$

The rigid-chain-limit model of Russell et al. [58] is used for specifying D^{rd}:

Table 2
Parameters used for simulating $\langle k_t \rangle$ based on a chain-length-dependent model

Experiment code	Exp1	Exp2	Exp3
[M] (M)	0.467	0.436	0.447
k_p ($M^{-1}\,s^{-1}$)	89,800	90,900	90,500
k_{tr} ($M^{-1}\,s^{-1}$)	10.6	10.73	10.68
fk_d[I] ($M\,s^{-1}$)	4.55×10^{-9}	1.93×10^{-8}	1.38×10^{-7}
p	0.25	0.25	0.25

Other significant parameters such as the initial and final fractional conversion and the radical concentration are given in Table 1, with other values adapted from the literature.

$$D^{\mathrm{rd}} = \frac{1}{6} k_p [\mathrm{M}] a^2 \tag{15}$$

where a is the root-mean-square end-to-end distance per square root of the number of monomer units in a polymer chain. The value a was taken as those suggested from earlier high-conversion studies [58]. In the present case of low conversion, the predicted relaxation kinetics are not significantly affected by reaction-diffusion, as expected, since this is only significant when centre-of-mass diffusion is slow (even for a system with a very high k_p such as acrylamide).

4.2. Diffusion coefficients

To specify the chain-length variation of the self-diffusion coefficient D_i^{com} for the diffusion coefficient of polar monomer in monomer/polymer solution, a scaling law was assumed:

$$\frac{D_i(w_p)}{D_{\mathrm{mon}}(w_p)} \approx i^{-u} \tag{16}$$

Fitting of extensive data for a series of different monomer–polymer systems has yielded the empirical relation [59–61]:

$$u = 0.66 + 2.02 w_p \tag{17}$$

This expression, while purely empirical, is consistent with literature studies of oligomer diffusion (except for possibly near $w_p = 0$). This gives close to the frequently observed limiting behavior of scaling as $u = 1/2$ as observed for many non-polar species at zero w_p, and approaching the $u = 2$ scaling suggested by reptation [62] at high w_p. The diffusion of AAm oligomers in water, as a function of its molecular weight and of w_p, has not been studied, and it is naïve to directly assume that the unusual properties of this polar species would allow the scaling laws to hold true.

The diffusion characteristics of similar hydrophilic species, hydroxylethylmethacrylate (HEMA), have been extensively investigated [61] for monomeric and oligomeric species as a function of w_p. The empirical scaling dependence that was found to be an adequate fit for styrene and MMA was also found to provide an adequate fit for HEMA. Due to the physical similarities between HEMA and AAm, an assumption was made that the diffusion behavior of the monomeric and oligomeric species would be similar. Although this assumption is likely to be imperfect due to different degrees of hydrogen bonding between the monomers, HEMA is the best model currently available. For initial investigation the D_{mon} for AAm was assumed to be equal to that of HEMA providing a foundation to estimate $D_i(w_p)$.

4.3. Simulating $\langle k_t \rangle$

The value for $\langle k_t \rangle$ was predicted based on the weight fraction range over which exp1, exp2 and exp3 γ-relaxation

experiments were conducted. The initial values used to predict $\langle k_t \rangle$ are presented in Table 2. Parameters that are justifiably open to some adjustment are the exponential scaling factor for predicting $D_i(w_p)$ in Eq. (16), p, D_{mon} and the k_p values for monomeric through to pentameric radicals.

The zero weight fraction value of the empirical scaling relationship defined by Eq. (16) has been shown to accept a scaling value lower than 0.66 [59,60]. In particular, the zero weight fraction data in those studies did not fit well to the global fit provided by Eq. (16): a value of 0.5 is perhaps more appropriate at $w_p = 0$. This could perhaps be because those data were measured at concentrations below c^*, the polymer concentration at which chain overlap becomes significant. It was found here that a value of 0.50 provided the most adequate fit for the experimental AAm $\langle k_t \rangle$ data (Table 3). It should be emphasized that this exponent (0.66 versus 0.5) is not an a priori relationship, and allows for some variation of the value. It is noted that the 0.5 exponent is consistent with the 'composite model' of Russell and co-workers [63]. Fig. 7 shows the experimentally determined $D_i(w_p)$ values for dimeric and tetrameric species and the estimated fits using scaling factors of 0.66, 0.50 and 0.40; it can be seen that a scaling factor as low as 0.40 still provides an adequate fit.

A D_{mon} value for AAm was provided by scaling the ratio of the molecular weight for each species, to the power of 1/2, against the D_{mon} value for HEMA. This returned a D_{mon} for AAm (at 50 °C) of 1.32×10^{-9} m^2 s^{-1}. The predicted $\langle k_t \rangle$ values found using this scaled D_{mon}, with a exponential scaling value of $u = 0.50$ for $D_i(w_p)$, are shown in Table 3 and Fig. 8. The predicted values of the termination rate coefficients using a zero w_p scaling coefficient of 0.50 correspond reasonably well (within at most a factor of 3) with the experimental data across this range.

The value of the diffusion coefficient for AAm is on the lower limit of the range for monomeric diffusion coefficients at $w_p = 0$ (e.g. D_{mon} values for methyl methacrylate and butyl methacrylate at $w_p = 0$ are 6.4×10^{-9} and 3.8×10^{-9} m^2 s^{-1}, respectively, at 40 °C [60]). This small diffusion coefficient for AAm compared to those for monomers of similar size that do not extensively hydrogen bond with their solvent is the primary reason for the low values of the predicted average termination rate coefficients compared with those of the non-hydrogen bonding systems. A sensitivity analysis illustrates how the predicted values for $\langle k_t \rangle$ depend on the value for D_{mon}. Table 3 shows calculations in which the value of D_{mon} is increased by a factor of 5, i.e. roughly to that of MMA at 40 °C. This calculation yields a value of $\langle k_t \rangle$ that is similar to those of styrene and MMA. The calculated value of $\langle k_t \rangle$ for this system shows an approximately linear dependence on D_{mon} for this system.

The sensitivity of the value for the primary k_p was also examined (Table 3), because k_p for AAm is very high (as are those of acrylates) compared to styrene and methyl methacrylate. The values returned for the $\langle k_t \rangle$ using k_p ten times slower are about three times larger; this is consistent with the observation that for styrene, with a low k_p (236 M^{-1} s^{-1} at 50 °C [64]), exhibits a $\langle k_t \rangle$ of about 2×10^8 M^{-1} s^{-1} with the same model, a value which is also consistent with experiment [11]. This is similarly seen for methyl methacrylate, which has a relatively low k_p and a high $\langle k_t \rangle$.

Although the calculated dependence of $\langle k_t \rangle$ on k_p is fairly strong here, the sensitivity analysis shown in Table 3 shows that the dominant contributor to the predicted low $\langle k_t \rangle$ values is the low value of D_{mon}. The polarity of each species, which can strongly affect $D_{mon}(w_p)$ and $D_i(w_p)$, fits accordingly for this trend, and as mentioned above strongly shapes the outcome of chain-length-dependent kinetic simulations. This is because the mobility of the short-chain radicals (which dominate termination) is slow for AAm (due to the low D_{mon}) and will be further reduced as the AAm chains undergo propagation. In addition to the sensitivity of the apparent overall k_p, $k_{p,1\text{-mer}}$ and $k_{p,5\text{-mer}}$ were altered, and it is observed that the returned values for $\langle k_t \rangle$ change only slightly when compared to the sensitivity to the overall apparent k_p.

Butyl acrylate, like acrylamide, has a very large k_p [65,66], and the model given above with the measured values for k_p and transfer [42] also yields a relatively low $\langle k_t \rangle$

Table 3
The dependence of the predicted value for $\langle k_t \rangle$ (M^{-1} s^{-1}) calculated from the chain-length-dependent model on the value of D_{mon}, on the empirical scaling factor u used to predict $D_i(w_p)$ from D_{mon} (Eq. (16)), on the apparent k_p, $k_{p,1\text{-mer}}$, $k_{p,5\text{-mer}}$ and on putting $k_{tr} = 0$

Experiment code	Exp1	Exp2	Exp3
γ-relaxation values ($\langle k_t \rangle$ M^{-1} s^{-1})	3×10^7	1×10^7	8×10^6
$u = 0.66$	7.7×10^6	7.8×10^6	8.4×10^6
$u = 0.50$	2.3×10^7	2.4×10^7	2.6×10^7
D_{mon} (m^2 s^{-1}) $= 1.32 \times 10^{-9}$	3.1×10^7	3.2×10^7	3.6×10^7
D_{mon} increased by factor of 5	1.2×10^8	1.3×10^8	1.5×10^8
Apparent k_p/10	7.3×10^7	7.6×10^7	8.9×10^7
$k_{p,1\text{-mer}} = 0.1 \times k_{p,app}$	2.4×10^7	2.5×10^7	2.7×10^7
$k_{p,1\text{-mer}} = 10 \times k_{p,app}$	2.3×10^7	2.3×10^7	2.6×10^7
$k_{p,5\text{-mer}} = 0.1 \times k_{p,app}$	2.4×10^7	2.4×10^7	2.7×10^7
$k_{p,5\text{-mer}} = 10 \times k_{p,app}$	2.3×10^7	2.4×10^7	2.6×10^7
$k_{tr} = 0$	3.7×10^6	6.0×10^6	1.14×10^7

The input parameters used for the predictions are taken from γ-relaxation experiments and previous studies on the apparent k_p.

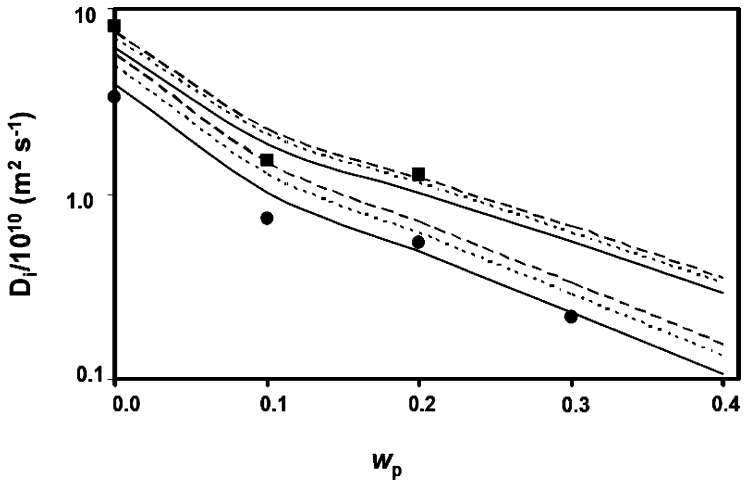

Fig. 7. Experimental data for dimeric (●) and tetrameric (■) HEMA oligomers as a function of the weight fraction polymer. The fitted lines represent predictions of D_i based on the exponential scaling relationship (Eq. (16)) using values of 0.66 (solid), 0.50 (dotted) and 0.40 (dashed).

(1.5×10^7 M^{-1} s^{-1}); a critical survey of the literature [10] has not revealed any reliable values for $\langle k_t \rangle$ for this monomer. However, for butyl acrylate, one cannot make meaningful comparison of $\langle k_t \rangle$ values predicted with the present model because termination in butyl acrylate is strongly affected by mid-chain radicals formed by transfer to polymer [67]. This is supported by the observed low termination rate coefficients for dodecyl acrylate [68], which is expected to diffuse relatively slowly, and to involve a large fraction of mid-chain radicals (although it is possible that a large fraction of mid-chain radicals might form during the polymerization of AAm, there appears to be no evidence in the literature for this). These calculations suggest that the factors governing the apparent termination rate coefficients of the acrylates are different from those AAm, styrene and methyl methacrylate, for none of which is there evidence of the formation of mid-chain radicals. The low D_{mon} for AAm is the greatest contributor to the slower termination rate coefficient, rather than the fast k_p which it shares with the acrylates.

The predicted variation in $\langle k_t \rangle$ with w_p is weaker than that observed. This may imply that the scaling of the diffusion coefficients with w_p for this very polar monomer are not well predicted by Eq. (16). However, an alternative physically reasonable explanation for the deviation between data at the lowest w_p and the remaining data is that the lowest w_p point occurs before c^* (and thus the 0.5 value of the zero w_p scaling coefficient is appropriate here), but the other data (above c^*) are better predicted by using the 0.66 coefficient. Given the uncertainties in several of the input parameters (e.g. p, D_{mon}, the scaling parameters, and the strong sensitivity of k_p to exact experimental conditions), it is believed that the predicted $\langle k_t \rangle$ values adequately model the observed data.

To assess the contribution of transfer to monomer, the k_{tr} value was set to zero, making termination strictly by

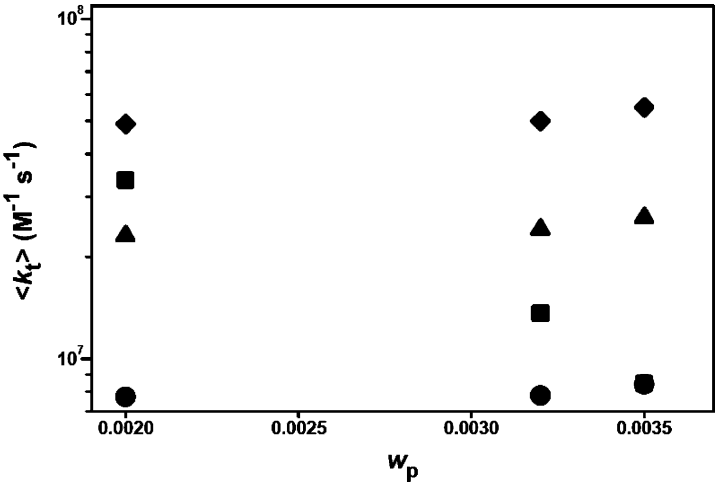

Fig. 8. The $\langle k_t \rangle$ values predicted from the chain-length-dependent model with variations based on the exponential scaling relationship used to predict $D_i(w_p)$ (Eq. (16)). Experimental $\langle k_t \rangle$ values from the γ-relaxation experiments (■), and calculated using scaling values of 0.66 (●), 0.50 (▲) and 0.40 (◆).

combination of two propagating radicals. The values returned for the $\langle k_t \rangle$ were at least an order of magnitude lower than those found with a realistic k_{tr} value: absolute values are shown in Table 3. Using $k_{tr}=0$, combined with the relatively high apparent k_p, will create a large population of long chain species, which as we have shown will drastically lower the $\langle k_t \rangle$ value for any given range of conversion. The experimental $\langle k_t \rangle$ data cannot be reproduced without the presence of populations of short chains generated by chain transfer to monomer, which indicates that transfer to monomer plays a very significant part in the kinetics of AAm polymerization, at least at low conversion. As mentioned, the experimentally calculated C_M value has a degree of uncertainty associated with it, which translates to upper and lower values for k_{tr} of 11.7 and 9.5 $M^{-1} s^{-1}$, respectively. These values return limits of 1.24×10^7 and 1.13×10^7 $M^{-1} s^{-1}$ when used to predict the $\langle k_t \rangle$ for the conditions described for exp1, which is small but significant and highlights, as does setting k_{tr} to zero, the sensitivity of $\langle k_t \rangle$ of a fast propagating system to C_M.

The observed sensitivities to the lowest k_p and to k_{tr} indicate that termination events in this case are largely insensitive to the shortest propagating radicals, while termination is largely controlled by chain transfer to monomer.

5. Conclusions

Average termination rate coefficients for the aqueous free-radical polymerization of AAm were measured by γ-relaxation experiments at 50 °C. These experimental values of $\langle k_t \rangle$ were relatively low when compared to those of common organic phase free radical polymerization systems. The measured $\langle k_t \rangle$ values were well predicted using a model for chain-length-dependent termination. The value for D_{mon} of AAm at 50 °C needed for this model was not available in the literature, and thus was adapted from that of a similarly hydrophilic system, HEMA, scaled based on the respective molecular weight for each monomer. In addition, the method used to provide $D_i(w_p)$ for AAm oligomers, which relies on an exponential scaling factor with degree of polymerization, was found to provide better agreement for the $\langle k_t \rangle$ using a value for the zero w_p scaling exponent slightly different from that provided by the literature at higher w_p (but within acceptable accord), namely 0.50 rather than 0.66, an exponent consistent with Russell's 'composite model' [63].

The chain transfer to monomer rate coefficient, k_{tr}, was measured using the chain-length-distribution method [20] taking SEC band broadening into account [21,22]. The value of C_M ($=k_{tr}/k_p$) so obtained was 1.2×10^{-4} ($\pm10\%$) at 50 °C.

The model quantitatively showed that the relatively high value for k_p and, more importantly, the relatively slow diffusion coefficients (D_{mon} and $D_i(w_p)$) are responsible for the low value of $\langle k_t \rangle$. Reducing the apparent k_p by a factor of ten significantly increased the $\langle k_t \rangle$ value. The model was highly sensitive to the value of k_{tr}; $\langle k_t \rangle$ dropped substantially with k_{tr} set to zero. This indicates that transfer to monomer is an important source of short chain radicals under such conditions.

This is the first successful application of the full chain-length-dependent termination model to any aqueous phase system. The chain-length-dependent treatment for predicting $\langle k_t \rangle$ gives very reasonable accord with the absolute values of $\langle k_t \rangle$ seen experimentally for this non-polar monomer, and is thus consistent with the assumptions of the diffusion-controlled model for termination.

Acknowledgements

We gratefully acknowledge the support of the Australian Research Council's Linkage program, and financial support of Life Therapeutics Pty. Ltd, as well as stimulating discussions with Drs David Solomon and David Ogle of that company. The support of the Australian Institute for Nuclear Science and Technology is greatly appreciated, as is the collaboration of David Sangster on the γ-radiolysis studies. The Key Centre for Polymer Colloids was established and supported under the ARC's Research Centres Program.

References

[1] Molyneux P. Water-soluble synthetic polymers: properties and behaviour. Tallahassee: CRC Press; 1983.
[2] Patras G, Qiao GG, Solomon DH. Macromolecules 2001;34:6396.
[3] Klein J, Conrad K-D. Makromol Chem 1980;181:227.
[4] Ganachaud F, Monteiro MJ, Gilbert RG. Macromol Symp 2000; 150/151:275.
[5] Kuchta F-D, Van Herk AM, German AL. Macromolecules 2000;33: 3641.
[6] Lacík I, Beuermann S, Buback M. Macromolecules 2001;34:6224.
[7] Lacik I, Beuermann S, Buback M. Macromolecules 2003;36:9355.
[8] Lacik I, Beuermann S, Buback M. Macromol Chem Phys 2004;205: 1080.
[9] Seabrook SA, Tonge MP, Gilbert RG. J Polym Sci, Part A: Polym Chem 2005;43:1357.
[10] Barner-Kowollik C, Buback M, Egorov M, Fukuda T, Goto A, Olaj OF, et al. Prog Polym Sci 2005;30:605.
[11] Buback M, Egorov M, Gilbert RG, Kaminsky V, Olaj OF, Russell GT, et al. Macromol Chem Phys 2002;203:2570.
[12] Shipp DA, Solomon DH, Smith TA, Moad G. Macromolecules 2003; 36:2032.
[13] Vana P, Davis TP, Barner-Kowollik C. Macromol Rapid Commun 2002;23:952.
[14] Lansdowne SW, Gilbert RG, Napper DH, Sangster DF. J Chem Soc, Faraday Trans 1 1980;76:1344.
[15] Napper DH, Gilbert RG. In: Allen GA, Bevington JC, Eastmond GC, editors. Comprehensive polymer science. Oxford: Pergamon; 1989. p. 171.
[16] Adams ME, Russell GT, Casey BS, Gilbert RG, Napper DH, Sangster DF. Macromolecules 1990;23:46240.

[17] Russell GT, Gilbert RG, Napper DH. Macromolecules 1993;26:3538.
[18] Benson SW, North AM. J Am Chem Soc 1962;84:935.
[19] Russell GT, Gilbert RG, Napper DH. Macromolecules 1992;25:2459.
[20] Clay PA, Gilbert RG. Macromolecules 1995;28:552.
[21] Castro JV, van Berkel KY, Russell GT, Gilbert RG. Aust J Chem 2005;58:178.
[22] van Berkel KY, Russell GT, Gilbert RG. Macromolecules 2005;38: 3214.
[23] Candau F, Leong YS, Fitch RM. J Polym Sci, Polym Chem Ed 1985; 23:193.
[24] O'Donnell JH, Sangster DF. Principles of radiation chemistry. London: Edward Arnold; 1970.
[25] Currie DJ, Dainton FS, Watt WS. Polymer 1965;6:451.
[26] Rabek JF. Experimental methods in polymer chemistry. New York: Wiley; 1980.
[27] Rollings JE, Bose A, Caruthers JM, Tsao GT, Okos MR. In: Craver CD, editor. Aqueous size exclusion chromatography. Washington, DC: American Chemical Society; 1983. p. 345.
[28] Kulicke W-M, Kniewske R, Klein J. Prog Polym Sci 1982;8:373.
[29] Heuts JPA, Davis TP, Russell GT. Macromolecules 1999;32:6019.
[30] Shortt DW. J Liq Chromatogr 1993;16:3371.
[31] Russell GT. Macromol Theory Simul 1995;4:497.
[32] Russell GT. Macromol Theory Simul 1995;4:519.
[33] Russell GT. Macromol Theory Simul 1995;4:549.
[34] De Bruyn H, Gilbert RG, Ballard MJ. Macromolecules 1996;29:8666.
[35] Brandrup J, Immergut EH, Grulke EA, editors. Polymer handbook. New York: Wiley; 1999.
[36] Buback M, Garcia-Rubio LH, Gilbert RG, Napper DH, Guillot J, Hamielec AE, et al. J Polym Sci, Polym Lett Ed 1988;26:293.
[37] Buback M, Gilbert RG, Russell GT, Hill DJT, Moad G, O'Driscoll KF, et al. J Polym Sci, Polym Chem Ed 1992;30:851.
[38] Buback M, Egorov M, Feldermann A. Macromolecules 2004;37: 1768.
[39] van Berkel KY, Russell GT, Gilbert RG. Macromolecules 2003;36: 3921.
[40] Castro JA, Koester C, Wilkins C. Rapid Commun Mass Spectrom 1992;6:239.
[41] Tobolsky AV, Offenbach J. J Polym Sci 1955;16:311.
[42] Maeder S, Gilbert RG. Macromolecules 1998;31:4410.
[43] Nikitin AN. Macromol Theory Simul 1996;5:957.
[44] Stickler M, Meyerhoff G. Makromol Chem 1978;179:2729.
[45] Thickett SC, Gilbert RG. Polymer 2004;45:6993.
[46] de Kock JBL, van Herk AM, German AL. J Macromol Sci, Polym Rev 2001;C41:199.
[47] Russell GT. Aust J Chem 2002;55:399.
[48] Cardenas J, O'Driscoll KF. J Polym Sci, Polym Chem Ed 1976; 14:883.
[49] Cardenas J, O'Driscoll KF. J Polym Sci, Polym Chem Ed 1977;15: 1883.
[50] Tulig TJ, Tirrell M. Macromolecules 1981;14:1501.
[51] Soh SK, Sundberg DC. J Polym Sci, Polym Chem Ed 1982;20:1299.
[52] Olaj OF, Zifferer G, Gleixner G. Macromolecules 1987;20:839.
[53] Bamford CH. Eur Polym J 1989;25:683.
[54] Mahabadi HK. Macromolecules 1985;18:1319.
[55] Mahabadi HK. Macromolecules 1991;24:606.
[56] Gilbert RG, Russell GT. Chem Aust 1995;62:21.
[57] Dainton FS. J Chem Soc 1952;1533.
[58] Russell GT, Napper DH, Gilbert RG. Macromolecules 1988;21:2133.
[59] Piton MC, Gilbert RG, Chapman BE, Kuchel PW. Macromolecules 1993;26:4472.
[60] Griffiths MC, Strauch J, Monteiro MJ, Gilbert RG. Macromolecules 1998;31:7835.
[61] Strauch J, McDonald J, Chapman BE, Kuchel PW, Hawkett BS, Roberts GE, et al. J Polym Sci, Part A: Polym Chem Ed 2003;41:2491.
[62] de Gennes PG. J Chem Phys 1971;55:572.
[63] Smith GB, Russell GT, Heuts JPA. Macromol Theory Simul 2003; 12:299.
[64] Buback M, Gilbert RG, Hutchinson RA, Klumperman B, Kuchta F-D, Manders BG, et al. Macromol Chem Phys 1995;196:3267.
[65] Lyons RA, Hutovic J, Piton MC, Christie DI, Clay PA, Manders BG, et al. Macromolecules 1996;29:1918.
[66] Asua JM, Beuermann S, Buback M, Charleux B, Gilbert RG, Hutchinson RA, et al. Macromol Chem Phys 2004;205:2151.
[67] Nikitin AN, Hutchinson RA. Macromolecules 2005;38:1581.
[68] Buback M. Makromol Chem 1990;191:1575.